

Evaluation of the time-dependency of the mechanical parameters of conditioned cohesionless soils

Original

Evaluation of the time-dependency of the mechanical parameters of conditioned cohesionless soils / Bahrami, Nima; Carigi, Andrea; Todaro, Carmine. - In: TUNNELLING AND UNDERGROUND SPACE TECHNOLOGY. - ISSN 0886-7798. - 150:(2024). [10.1016/j.tust.2024.105828]

Availability:

This version is available at: 11583/2993417 since: 2024-10-15T13:44:10Z

Publisher:

Elsevier

Published

DOI:10.1016/j.tust.2024.105828

Terms of use:

This article is made available under terms and conditions as specified in the corresponding bibliographic description in the repository

Publisher copyright

Elsevier postprint/Author's Accepted Manuscript

© 2024. This manuscript version is made available under the CC-BY-NC-ND 4.0 license
<http://creativecommons.org/licenses/by-nc-nd/4.0/>. The final authenticated version is available online at:
<http://dx.doi.org/10.1016/j.tust.2024.105828>

(Article begins on next page)



Evaluation of the time-dependency of the mechanical parameters of conditioned cohesionless soils

Nima Bahrami^{*}, Andrea Carigi, Carmine Todaro

DIATI Tunneling and Underground Space Laboratory, Politecnico di Torino, 10129 Turin, Italy

ARTICLE INFO

Keywords:

EPB-TBM
Tunneling
Soil conditioning
Time-dependency
Foam
Flow rate

ABSTRACT

In tunneling technology, Earth Pressure Balance-Tunnel Boring Machine (EPB-TBM) technology operations require altering excavated soil rheology through soil conditioning, a vital aspect for optimal counterpressure control and soil extraction. This transformation is achieved by introducing additives like foam, and inherits its time-dependent behavior. Having observed a discrepancy in the stability of two foams generated with different flow rates, the core objective of research is exploring the influence of this parameter on time-dependency of mechanical properties of conditioned soil. This aspect is then studied also through a semi-quantitative analysis aimed to investigate correlations between the generation flow rates, the Foam Expansion Ratio, and used Foam Injection Ratio with the time-stability of conditioned soil properties.

1. Introduction

In the field of mechanized tunneling, a substantial portion of the market is occupied by Earth Pressure Balance-Tunnel Boring Machines (EPB-TBM). Ensuring efficient EPB-TBM operation necessitates to change the rheological properties of excavated soil to give a pulpy consistency for better pressure control within the bulk chamber and soil extraction through the screw conveyor. Among various conditioning agents, foam is the most important one. Since the bubbles strongly interact with the soil grains and the foam quality influences the conditioning process to a great extent, the assessment of the stability of foam is a key issue in the development of the soil conditioning design within the conditioned soil arises from the excavation cycle (Carigi et al., 2022).

The material excavated by the cutterhead spends a variable amount of time inside bulk chamber before being extracted by the screw conveyor. This duration can vary from about one hour to potentially several hours or days in cases where unforeseen excavation issues occur (Peila et al., 2008). Thus, gaining a deeper understanding of how foam properties influence the stability of conditioned soil could have significant impact on the job site management and safety.

The stability of foam in time is measured through the half-life time, which is given by EFNARC (EFNARC, 2005). Subsequently, some relationships between surfactant concentration, viscosity of the liquid generator, and foam stability have been investigated by other authors

(Carigi et al., 2022; Moll et al., 2020; Sebastiani et al., 2019; Zhang et al., 2015). Followingly, several authors have previously focused on the half-life test to assess the stability of foam (Galli and Thewes, 2019; Sebastiani et al., 2019; Zhao et al., 2021; Zhou and Yang, 2020). According to Wu et al. (2018), foam stability is strongly influenced by pressure, stating that higher pressure environments yield smaller and more uniform foam bubbles.

Thewes et al. (2012) states that, in half-life tests, the drained liquid mass depends on the choice of foaming agent and of the foam generator type. The outcomes were driven from the tests with four different foaming agents and two different foam generators, which were used to produce foam under atmospheric pressure. The employed foam guns were with different mechanical inserts for the creation of turbulences, and the properties of the foaming systems are extensively described in Budach (2012).

According to Budach and Thewes (2015), the type of foam gun and the selection of foaming agent product have a great influence on the drain time. In addition to two foam guns commonly used in practice, a third foam gun was installed on the foam generator which allows the production of foam with low flow rates. Consequently, a qualitative influence of different parameters, such as type of foam gun, volume flow of foam, pumping pressure, conditioning agent, foaming agent concentration, and FER, on the quality of the foam is presented (Budach and Thewes, 2015; Thewes and Budach, 2010).

Carigi et al. (2022), using half-life test, proved that along the Foam

^{*} Corresponding author.

E-mail addresses: nima.bahrami@polito.it (N. Bahrami), andrea.carigi@polito.it (A. Carigi), carmine.todaro@polito.it (C. Todaro).

Expansion Ratio (FER) range of 5 to 30, with the same foaming agent concentration, two distinct foam generator flow rates produce samples with sensible variation in the stability.

It is critical to highlight that the effect of foam generator flow rate on conditioned soil stability has not been investigated yet. This research aims to analyze how the flow rate of generation fluid affects the mechanical parameters of the conditioned soil and their stability in time, such as the slump value, the bulk density, and the Scissometric Index according to Carigi et al. (2020).

2. Materials and methods

2.1. Soil

In this research, the soil coming from a morain formation is used as the reference soil. The sample was obtained from a tunnel in Northern Italy. To verify the homogeneity of the sample, 6 grain size distributions were carried on. The grain size distributions and their average, analyzed following ASTM D6913-04 standard, are presented in Fig. 1. Moreover, the soil exhibited a density of 1.91 kg/L, with its natural water content (W_{natural}) estimated at 4.44 %, according to ASTM D2216-19 standard.

2.2. Foam

The foam was produced with a generator used in previous studies (Carigi et al., 2022; Peila et al., 2019; Vinai et al., 2007), with the scheme of Fig. 2 and Fig. 3. This generator allows to use different flow rates of the generation fluid (Q_L), in the following flow rate, varying from 2.8 L/min up to 10.0 L/min. Additionally, the foam generator can accurately control the quantities of air, water, and foaming agent in a generation cylinder with an internal diameter of 78 mm, and a length of 450 mm, full of glass fragments with an average diameter of 5 mm (Peila et al., 2008).

For the conditioning, a commercial conditioning agent with the following declared composition:

- Alcohols, C12-14, ethoxylated, sulfates, sodium salts ($c > 10\%$ – $< 20\%$) CAS: 68891-38-3;
- 5-chloro-2-methyl-2H-isothiazol-3-one and 2-methyl-2H-isothiazol-3-one ($c > 0.0002\%$ – $< 0.0015\%$) CAS 55965-84-9.

The parameters that are commonly considered in soil conditioning design are mentioned in Table 1.

In the context of this research an additional parameter is considered,

namely, the flow rate (Q_L).

2.3. Half-life test

Generally, in the tunneling industry the stability of the generated foam is measured through the half-life test defined by EFNARC (EFNARC, 2005) and consists of measuring the time (t_{50}) needed for an 80-grams foam sample to drain half of its weight.

2.4. Conditioning set parameters

The optimal conditioning set parameters has been defined following the procedure suggested by Peila et al. (2019). The foam was produced by using two different flow rates, specifically denoted as the maximum flow rate ($Q_L = Q_{L(\text{max})} = 10.0$ L/min) and the minimum flow rate ($Q_L = Q_{L(\text{min})} = 2.8$ L/min), with the foaming agent concentration (c_f) of 2.0 %. Two different values of Foam Expansion Ratios, 8 and 15, were used. Using this parameter, it was set the optimal conditioning by varying the amount of added water and foam. The results are presented in Table 2.

For each type of generated foam, the pressure drop (ΔP) registered in the mixing column, between the generator inlet pressure and generator outlet pressure (Fig. 2), were measured and are reported in Table 2.

2.5. Conditioned soil mechanical properties assessment

In order to evaluate the changes in mechanical properties of the conditioned soil over time the workability, bulk density, and shear strength, were chosen to be investigated accordingly to Carigi (2023). Other tests were used by Carigi et al. (2020), such as the direct shear test (ASTM D3080-04), the modified Proctor test (AASHTO T193), and the rotational mixer test (Martinelli, 2016). The direct shear test was excluded since it requires to remove all the soil fraction above 4.75 mm, changing the nature of the soil itself. The Proctor test was not useful for this research since it produces results only in the late stage of the conditioned soil evolution, beyond the scope of this paper. Lastly, the rotational mixer test was not adopted due to the logistic constraints in its operation linked to the huge amount of soil needed to perform a single test. The workability was evaluated through the slump test, performed according to Peila et al. (2019). The bulk density was measured through direct approach by weighting a sample of 2 dm³. In particular, differently from Yee et al. (2018), in order not to affect the sample dimension, the test was not associated with the determination of the dry bulk density, which would require to dry the sample. The shear strength was measured with a modified vane test, as presented in Carigi et al. (2020),

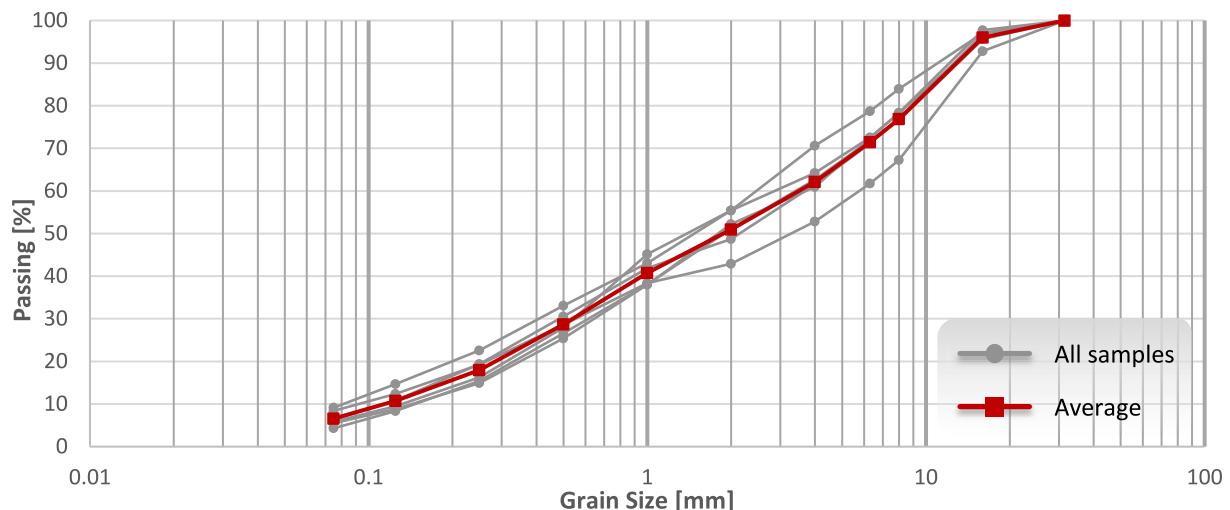


Fig. 1. Grain size distribution curve.

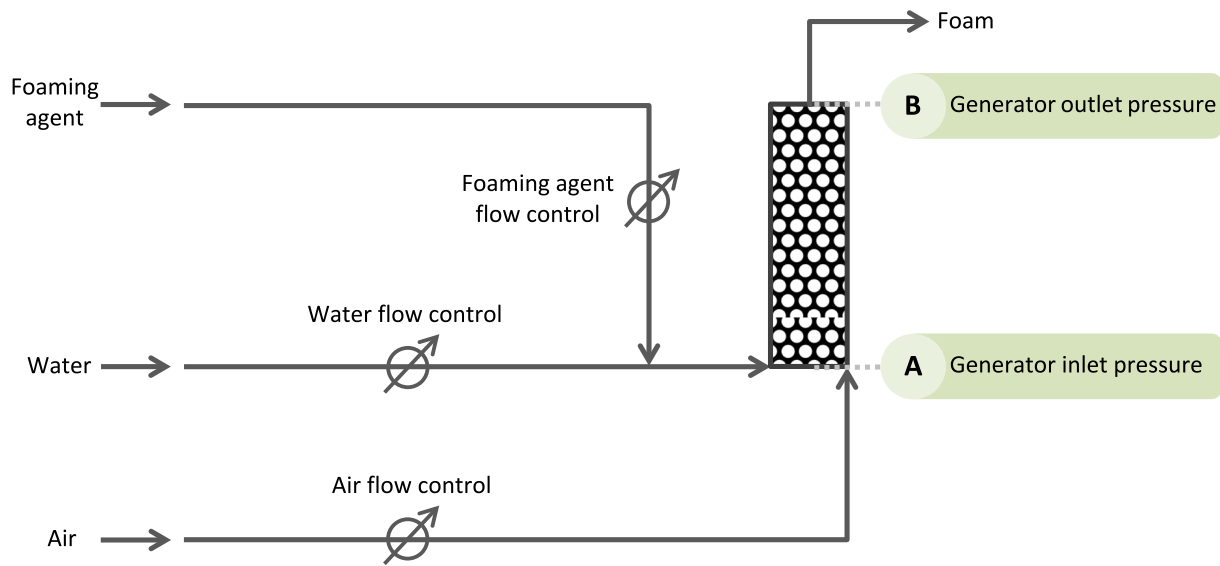


Fig. 2. Foam generation process scheme (Peila et al., 2008).



Fig. 3. Left: Laboratory scale foam generator at TUSC laboratory (Martinelli, 2016); Right: Generation cylinder (Peila et al., 2008).

Table 1
Foam conditioning parameters.

| Parameter | Unit | Formula |
|---------------------------------------|------|-------------------------------------------------------------------|
| Foam Injection Ratio (FIR) | % | $\frac{V_{foam}}{V_{soil}} \cdot 100$ |
| Foam Expansion Ratio (FER) | – | $\frac{V_{liquid\ generator}}{V_{foam}}$ |
| Foaming agent concentration (c_f) | % | $\frac{V_{conditioning\ agent}}{V_{liquid\ generator}} \cdot 100$ |
| Total water content (w_{total}) | % | $\frac{M_w}{M_s} \cdot 100$ |
| Added water content (w_{added}) | % | $w_{total} - w_{natural}$ |

which is based on the estimation of the Scissometric Index (I_{sc}). This parameter, despite being procedurally determined like undrained cohesion in the vane test, has been renamed here to avoid confusion due to the fact that the conditioned soil does not have cohesion itself.

2.6. Semi-quantitative analysis

Segmented Regression Analysis is employed to perform a semi-

Table 2
Conditioning set parameters for main test campaigns.

| Parameter | 9 | | | |
|------------------|-------------------|---------|--------------------|---------|
| | $Q_L (min) = 2.8$ | | $Q_L (max) = 10.0$ | |
| w_{total} (%) | 8 | 15 | 8 | 15 |
| Q_L (L/min) | 0.025 | 0.025 | 0.025 | 0.025 |
| FER (–) | 0.225 ± | 0.325 ± | 0.300 ± | 0.425 ± |
| ΔP (bar) | – | 20 | 20 | 20 |
| FIR (%) | 30 | 30 | 30 | 30 |
| | 40 | 40 | 40 | 40 |
| | 50 | 50 | 50 | 50 |

quantitative analysis of the collected data from slump test, density test, and vane shear test throughout all the test campaigns. The analysis focuses on exploring potential correlations among the outcomes in relation to distinct flow rates, Foam Expansion Ratios (FER), and Foam Injection Ratios (FIR). The chosen method is a statistical technique employed to model relationships between variables in situations where there are distinct breakpoints or segments in the data.

The initial step is Data Splitting, where the obtained results from the test campaigns are divided into two series. The breakpoint is changed to

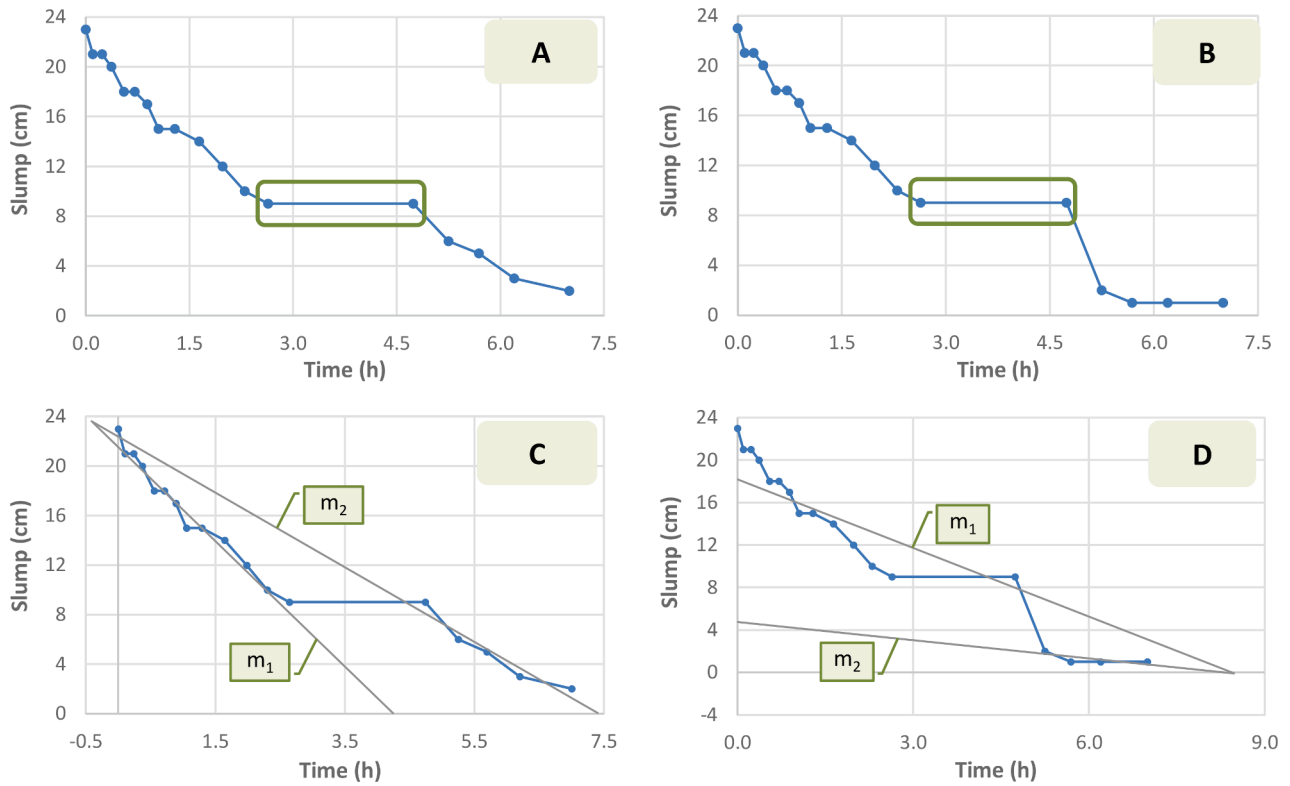


Fig. 4. Gap in the empirical results.

all possible positions in the series with the constraint to leave at least 3 data point for each series. Then, a linear regression is carried out for each series and the values of slope and intercept for each set are separately estimated through least squares method. Specifically, the objective is to minimize the sum of squared differences between the observed values and the predictions generated by the respective linear models. Being N the number of total observations, n the position of breakpoint, S_i and S_j the observations respectively on the first and second series, the optimization process is aimed at finding the optimal values for lines parameters, denoted as m_1 , q_1 , m_2 , and q_2 to minimize the following expression:

$$\left[\sum_{i=1}^n (S_i - (m_1 t_i + q_1))^2 + \sum_{j=n+1}^N (S_j - (m_2 t_j + q_2))^2 \right]$$

Having successfully minimized the abovementioned expression, the associated line parameters are preserved. The process is iterated for all the values of n between 3 and $N-3$. Then, the breakpoint position that minimizes squared error is selected to preliminary define the best fitting model.

Due to logistic limitations in laboratory operations, it was not feasible to conduct tests continuously at consistent intervals over a 24-hour period. Hence, gaps in the empirical results are present, as shown in Fig. 4(A, B). These gaps can induce some errors, as shown in

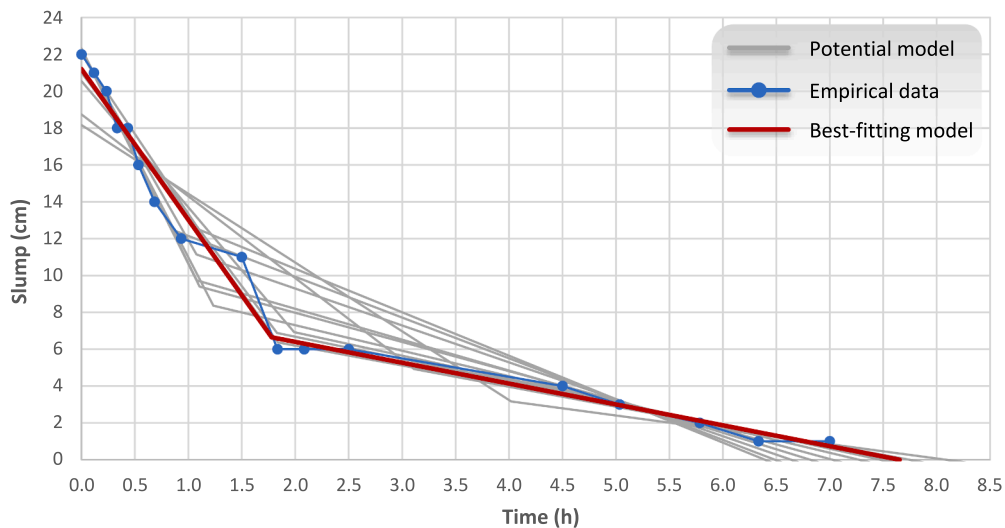


Fig. 5. Best-fitting model with the minimum sum of squared differences.

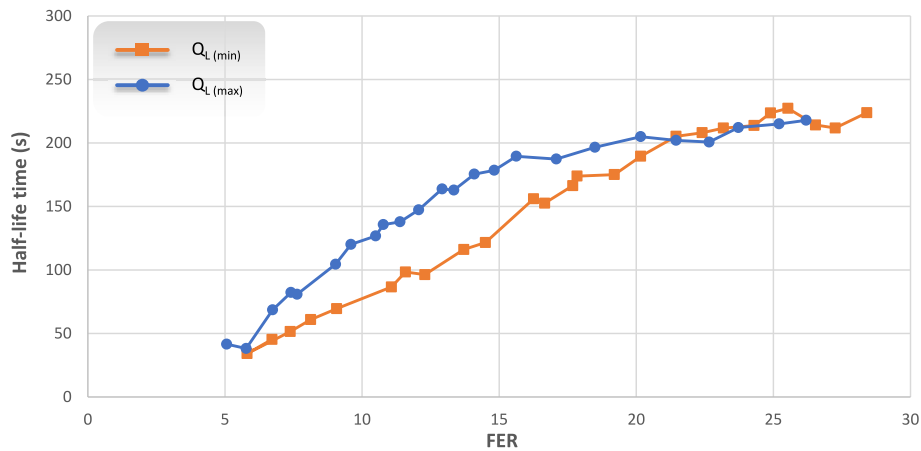


Fig. 6. Half-life time vs. FER for different foam generator flow rates.

Fig. 4(C, D), if the least squared regression optimization is carried on blindly. In such instances, some additional constraints on m_1 and m_2 have to be applied in order to guarantee that the chosen model has consistency with the observations.

In the instances of modeling anomalies two constraints are violated. Firstly, the interception of two lines is not permitted for $t < 0$. Additionally, having $m_2 > m_1$ cannot be considered as acceptable. The highlighted gap may create a situation where the blind application of the mathematical approach could become ineffective. Regarding density and vane shear tests, analogous considerations and the same constraints have to be imposed.

In Fig. 5 an example of the optimization for a test is shown. The observation series encompasses 17 data points, presented in blue. Then, all 12 potential models are presented in gray, and being anomalies absent, the best-fitting model for the given dataset is shown in red.

3. Results

3.1. Half-life tests versus foam generator flow rate

To verify the dependency of foam stability on the flow rate, samples were produced both with Q_L (min) and Q_L (max), and the results of half-life time values are presented in Fig. 6. The data show that there is a dependence of half-life time with the flow rate. It is possible to observe that there is a sensible difference between the two series (i.e. for FER = 13, the half-life time of the foam generated with Q_L (min) and Q_L (max), is 96 and 147 s, respectively, which shows an increment of around 50 %). This variation is more significant especially for the range of FER between 8 and 20.

3.2. Test campaign on conditioned soil

The results of the mechanical properties tests versus time are presented in this chapter within Fig. 7, from which it is possible to observe that by increasing the FIR, an increment of slump values, and a reduction in the gradient of flowability decay is produced. Furthermore, higher FER gives a less stable muck whose properties change faster.

With regard to slump test results, it is possible to observe that, especially for high values of FIR, the soil conditioned with low flow rate foam is more stable than the one conditioned with high flow rate foam.

3.3. Semi-quantitative analysis

The relationships between the slope and intersection of the lines parameters, explained in Chapter 2.6, versus Foam Injection Ratios (FIR) are presented in Fig. 8, Fig. 9, and Fig. 10.

4. Discussion on the results

4.1. Half-life test

The foam generated with high flow rate (Q_L (max)) appears to be more stable than the foam generated with low flow rate (Q_L (min)), as it can be seen in Fig. 6. This difference is particularly evident within the Foam Expansion Ratio range of 8 to 20. However, beyond FER = 20, the influence of flow rate diminishes, and the half-life times of the generated foams converge to nearly identical values. This phenomenon can be attributed to the fact that as the flow rate increases, smaller bubbles are generated and at the certain level the bubbles are very similar. Thus, results are in good agreement with those of Wu et al. (2018), who stated that when foam bubbles are smaller exhibit greater uniformity, resulting in a notably slower growth in bubble size over time. Regarding the foam degradation mechanisms, foam bubbles with uniform sizes are more stable due to less gas diffusion between bubbles.

4.2. Conditioned soil stability

Similarly to the results proven by Thewes et al. (2012), with increasing Foam Injection Ratio, the slump value will also increase. This trend is also visually illustrated in Fig. 7 A, B.

Generally, the conditioned soil with a lower Foam Expansion Ratio exhibits more stable properties over time, including flowability, lower bulk density, and reduced Scissometric Index (Fig. 7).

Moreover, generally for the same Foam Expansion Ratio, the conditioned soil with foam generated at minimum flow rate demonstrates greater stability than the conditioned soil with foam generated at maximum flow rate. The discrepancy is visually illustrated through utilization of dashed line for low flow rate (Q_L (min)), and solid line for high flow rate (Q_L (max)) in Fig. 7.

Comparing these findings with the ones of half-life tests, where generated foam at higher flow rate exhibits greater stability, the results seem counterintuitive. These variations could be attributed to the complex characteristics of the interaction between soil and foam during preparation and execution of the slump tests.

More specifically, the reason could be related to an aspect assessed by Thewes et al. (2012): smaller bubble size leads to a longer drainage time and consequently enhanced foam stability, but there is a critical lower limit for bubble dimensions. Beyond this limit, excessively small bubbles may potentially be smaller than the intergranular pores of the soil, having the possibility to migrate the foam will move accordingly to pressure gradients present in the excavation chamber and collect on top of it, factually reducing the amount of intergranular foam in the soil, and thus affecting the stability of foam-conditioned soil.

Furthermore, as the Foam Injection Ratio increases, the stability of the conditioned soil also increases in terms of flowability, bulk density, and shear strength of the conditioned soil.

4.3. Semi-quantitative analysis

The trends of m_2 and q_2 (Fig. 8, Fig. 9, and Fig. 10) show a complex behavior, which has more complex interpretation and may be affected by the uncertainties due to the abovementioned temporal gap in the tests (Fig. 4 A, B).

The variations between points in FER = 15 are more pronounced than FER = 8. Thus, it can be said that the influence of flow rate is less relevant for FER = 8. Moreover, with respect to Fig. 8, the trend of q_1 , that represents the initial value of slump after conditioning, shows a regular increment of the intercept point with FIR. Similarly, for bulk density and shear strength, the trends of q_1 (Fig. 9, and Fig. 10), show that as the FIR increases, the starting point decreases. This is mainly because the higher amount of foam is introduced to the soil, leading to reduced bulk density, and a reduced contact between soil grains. This result is in good agreement with the scientific literature (Mori et al., 2018; Wang et al., 2022). Conversely, the trend of q_2 of bulk density (Fig. 9) exhibits an almost steady behavior despite variations in Foam Injection Ratios.

Concerning the stability of the parameters, the coefficient m_1 (Fig. 8, Fig. 9, and Fig. 10) highlights a sensible difference for lower FIR, especially for FIR = 30, resulting a more rapid alteration in the properties of the material. Hence, modifying the flow rate of the generation liquid could regulate the speed of decay and reduce the necessity re-injecting foam during stoppage phases. These differences between flow rates are more significant for higher FER, while exhibiting similar behavior with slight variations in soil conditioned with lower FER.

5. Conclusions

Given the importance of optimization in conditioning set parameters design for EPB-TBM technology, research to investigate the effect of various conditioning factors on the characteristics of conditioned soil versus time was carried out. The study compared how different flow rates of the generation fluid in foam generation, that is related to the foam size and foam stability, influence the time-dependency of mechanical properties of the conditioned soil. The test campaign encompassed a wide range of conditioning set parameters and featured several specific tests, such as slump test, density test, and vane shear test.

The research stems from the concept that the half-life of foams generated with different conditions may be different. Hence, some tests have been carried out and confirmed that in the investigated case, foam

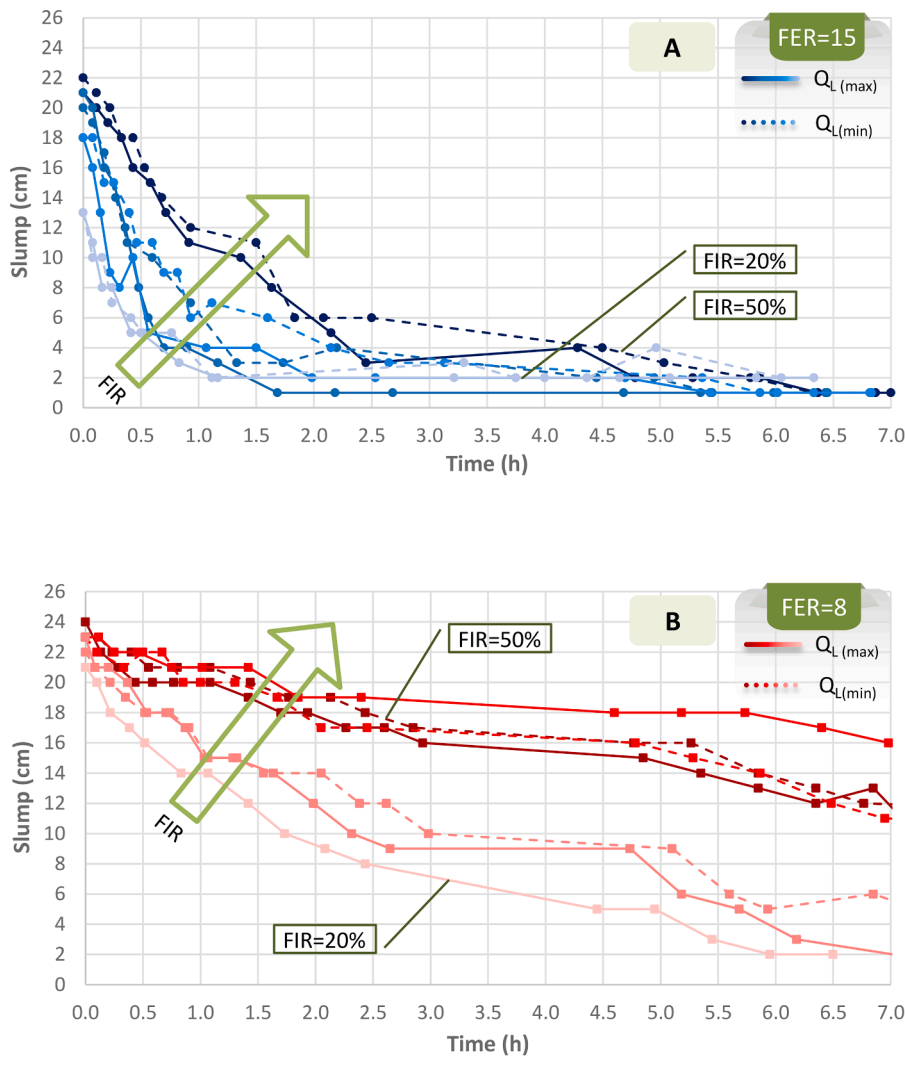


Fig. 7. Results for all main test campaigns (A, B: Slump test, C: Density test, D: Vane shear test).

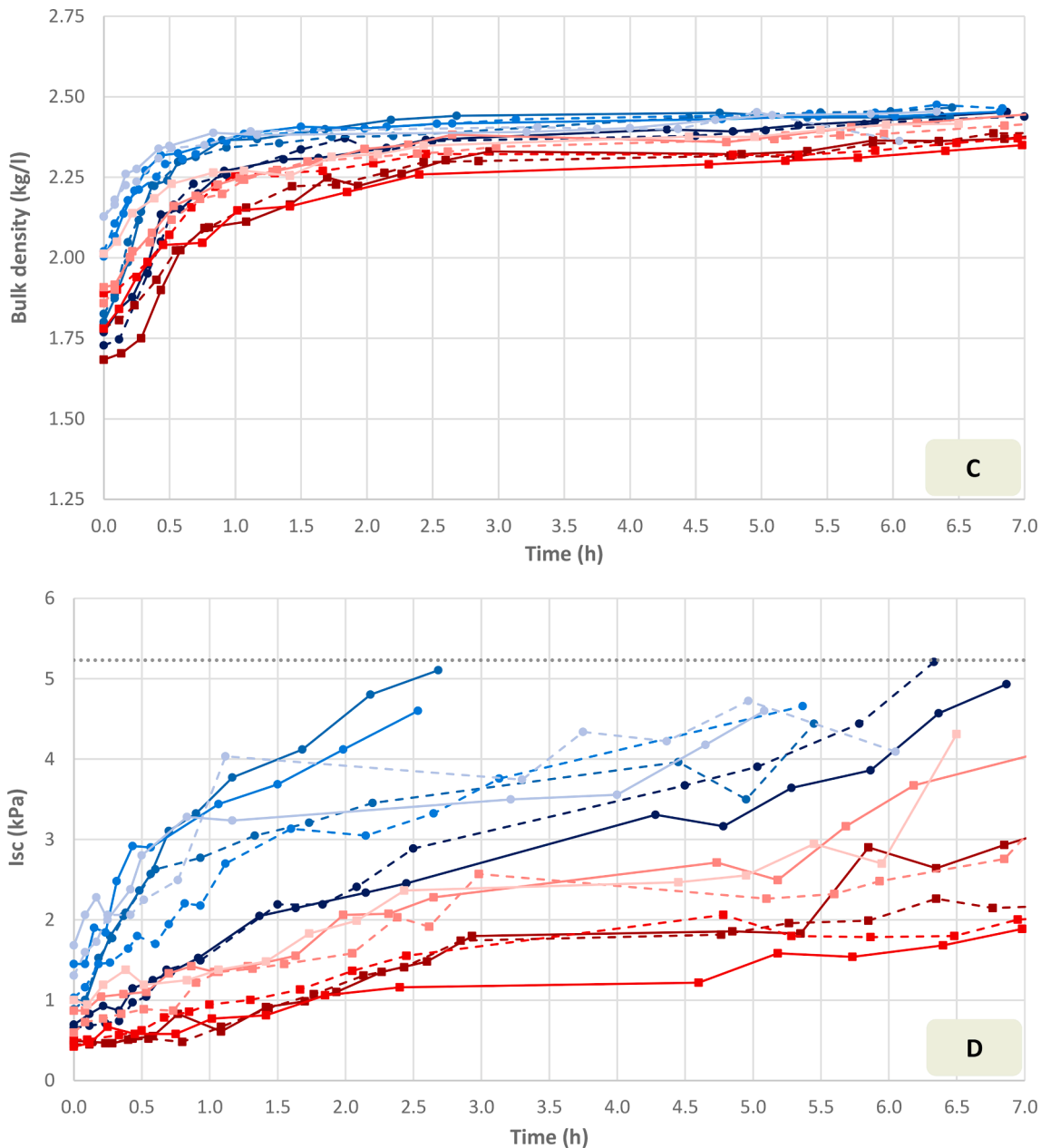


Fig. 7. (continued).

generated at high flow rate has greater stability compared to foam generated at low flow rate. This variation was particularly consistent up to Foam Expansion Ratio of 20.

The tests conducted on conditioned soil shown that differences are more pronounced in the outcome of slump tests, while remaining relatively slight in terms of density and vane shear tests. For FER = 15 the differences induced by the flow rate on the slump test accounted up to 3 cm as absolute difference between single values in the first hour, and differences up to 8 cm/h comparing the gradients on the semi-quantitative analysis. Similar results are evident also for bulk density (0.30 kg/dm³h), and the Scissometric Index (1.9 kPa/h). Considering the influence of workability on soil conditioning assessment, it is remarkable that, under identical conditioning set parameters (water content, type of conditioning agent and its concentration, FER, and FIR) but varying flow rates the results are different.

Additionally, a potential correlation between various conditioning set parameters through semi-quantitative analyses was searched for.

However, these results do not provide definitive conclusions, necessitating further research for validation and verification. Furthermore, additional soil types and conditioning agents may be tested in future development of the research.

The evaluation of how flow rate of the generation fluid influences the stability of conditioned soil has strong implications to real-world tunnel construction scenarios, as it may introduce the critical considerations regarding water, energy, and conditioning agent consumption. In fact, the use of these resources strongly depends on the efficiency with which the jobsite is managed, and a deeper understanding of the time evolution of properties of the conditioned soil in the excavation chamber may help to optimize the excavation process. Furthermore, the composition of conditioned soil under lower flow rates facilitates more stable and manageable material handling and muck removal over time.

Hence, optimizing flow rates of the generation fluid emerges as a strategic approach for enhancing efficiency, reducing resource consumption, and promoting sustainability in tunnel construction practices.

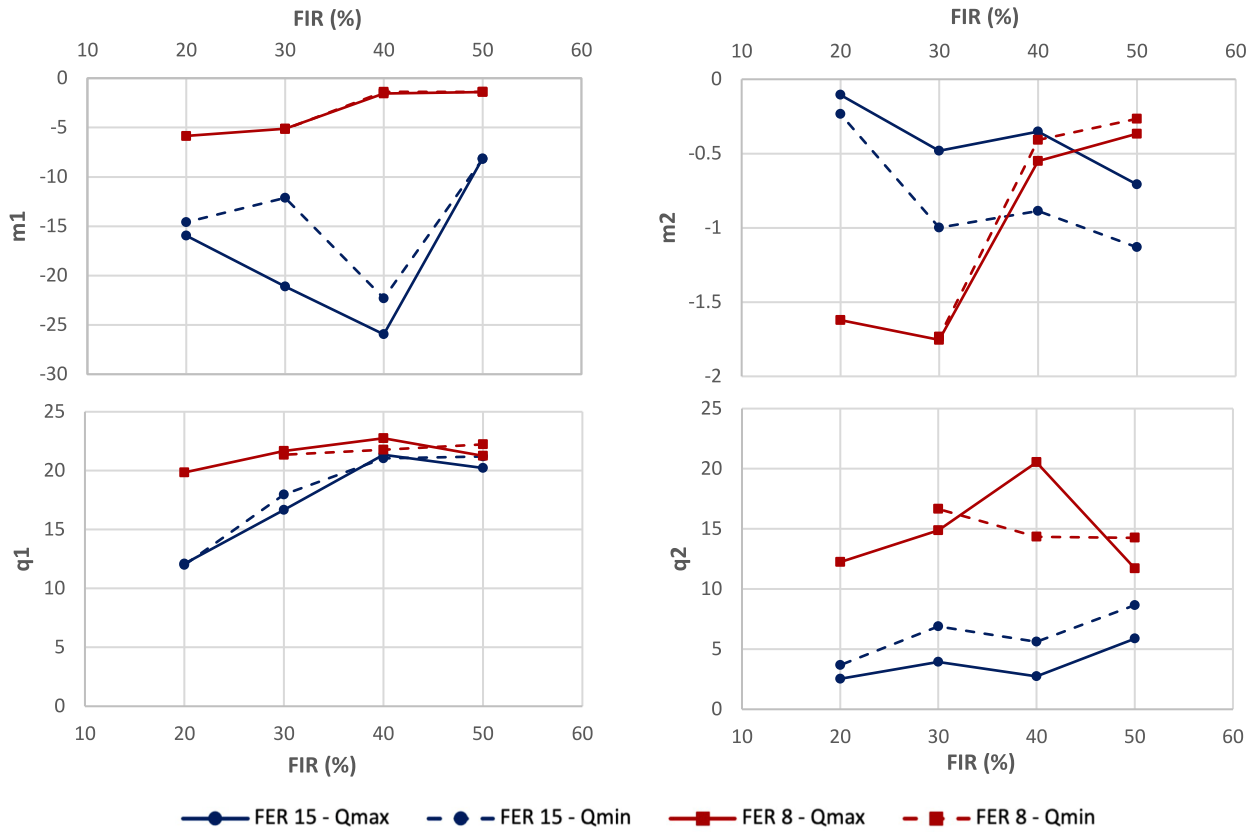


Fig. 8. Regression parameters for slump test.

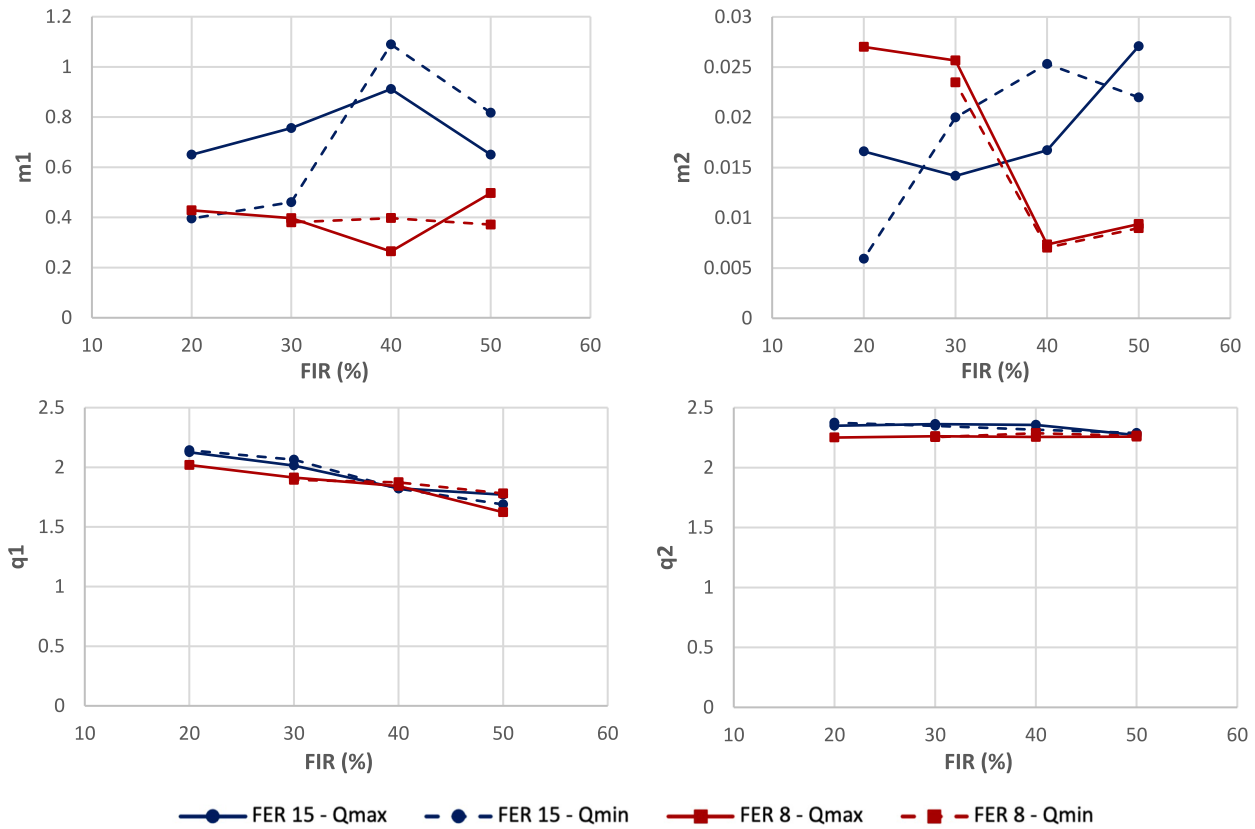


Fig. 9. Regression parameters for density test.

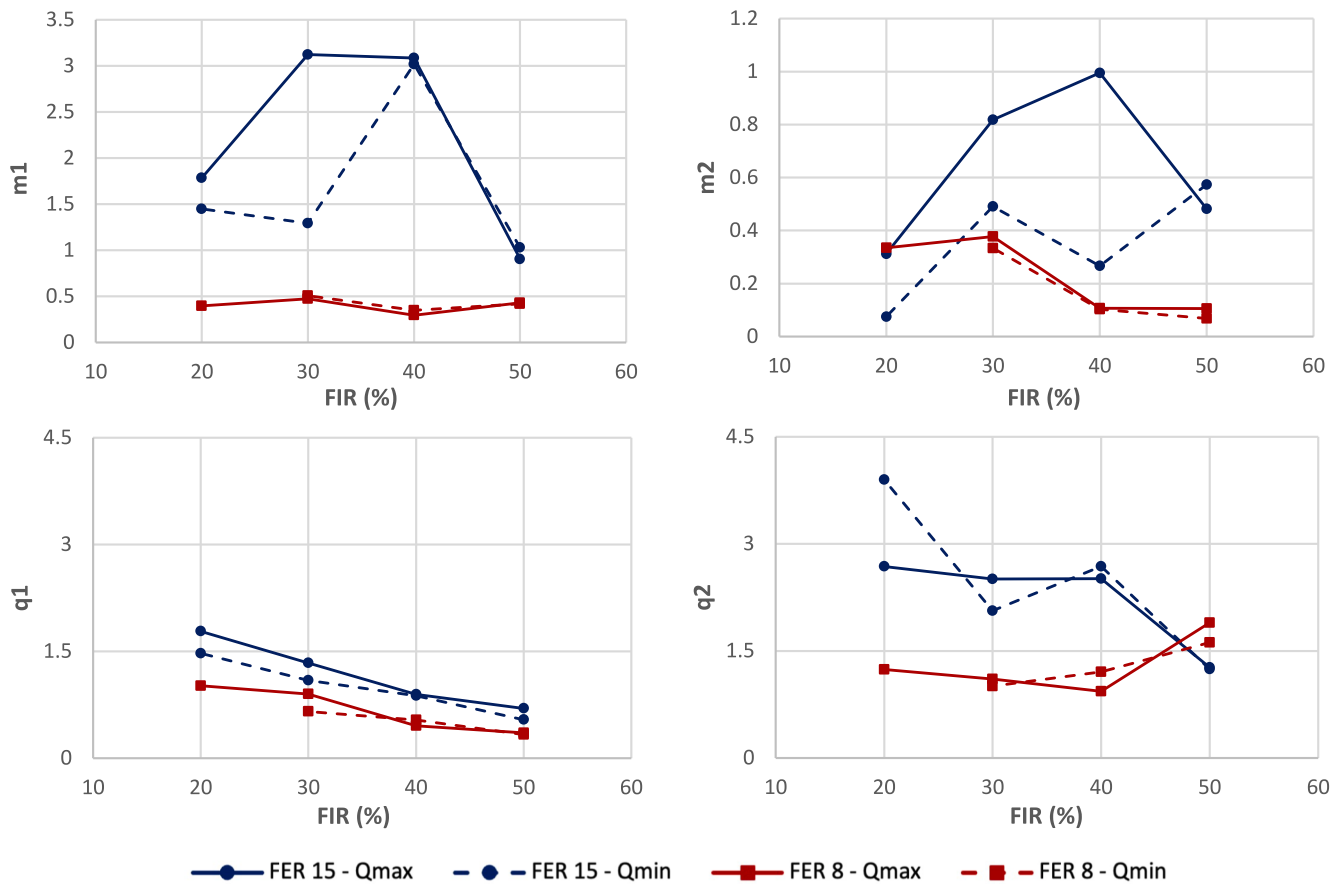


Fig. 10. Regression parameters for vane shear test.

The adoption of lower flow rates not only addresses environmental concerns but also brings tangible benefits in terms of reduced water usage, energy conservation, and enhanced cost-effectiveness.

Funding

This research was funded through contract 473/2023 of Department of Environment, Land and Infrastructure Engineering of Politecnico di Torino and by Dipartimento di Eccellenza 2023-2027 (15659 – 28 December 2022).

CRedit authorship contribution statement

Nima Bahrami: Writing – original draft, Investigation, Conceptualization. **Andrea Carigi:** Conceptualization, Investigation, Writing – original draft, Writing – review & editing. **Carmine Todaro:** Writing – original draft, Writing – review & editing.

Declaration of competing interest

The authors declare that they have no known competing financial interests or personal relationships that could have appeared to influence the work reported in this paper.

Data availability

Data will be made available on request.

Acknowledgments

The author acknowledges Professor D. Peila for suggestion and

guidance.

References

- AASHTO T193, 1993. Guide for Design of Pavement Structures. AASHTO: Washington, DC, USA, 1993.
- ASTM D2216-19, 2019. Standard Test Methods for Laboratory Determination of Water (Moisture) Content of Soil and Rock by Mass. ASTM International: West Conshohocken, PA, USA, 1990.
- ASTM D3080-04, 2012. Standard Test Method for Direct Shear Test of Soils Under Consolidated Drained Conditions. ASTM International: West Conshohocken, PA, USA, 1990.
- ASTM D6913-04, 2017. Standard Test Methods for Particle-Size Distribution (Gradation) of Soils Using Sieve Analysis. ASTM International: West Conshohocken, PA, USA, 1990.
- Budach, C., 2012. Untersuchungen zum erweiterten Einsatz von Erddruckschilden in grobkörnigem Lockergestein (Transl.: Investigations for extended use of EPBshields in coarse-grained soils). Ph.D. Thesis, Ruhr-Universität Bochum, Bochum, Germany.
- Budach, C., Thewes, M., 2015. Application ranges of EPB shields in coarse ground based on laboratory research. *Tunn. Undergr. Space Technol.* 50, 296–304. <https://doi.org/10.1016/j.tust.2015.08.006>.
- Carigi, A., Todaro, C., Martinelli, D., Peila, D., 2022. A More Comprehensive Way to Analyze Foam Stability for EPB Tunnelling—Introduction of a Mathematical Characterization. *Geosciences* 12 (5), 191. <https://doi.org/10.3390/GEOSCIENCES12050191>.
- Carigi, A., Todaro, C., Martinelli, D., Amoroso, C., Peila, D., 2020. Evaluation of the geo-mechanical properties recovery in time of conditioned soil for EPB-TBM tunneling. *Geosciences (switzerland)* 10 (11), 1–10. <https://doi.org/10.3390/GEOSCIENCES10110438>.
- Carigi, A., 2023. Time-dependency of mechanical properties of EPB-conditioned soil. Ph. D. Thesis, Politecnico di Torino, Torino, Italy.
- EFNARC, 2005. Specification and guidelines for the use of specialist products for Mechanized Tunnelling (TBM) in Soft Ground and Hard Rock, before extraction after extraction.
- Galli, M., Thewes, M., 2019. Rheological characterisation of foam-conditioned sands in EPB tunneling. *Int. J. Civ. Eng.* 17 (1), 145–160. <https://doi.org/10.1007/S40999-018-0316-X>.

- Martinelli, D., 2016. Mechanical Behaviour of Conditioned Material for EPBS Tunnelling. Ph.D. Thesis, Politecnico di Torino, Torino, Italy. <https://doi.org/10.6092/polito/p orto/2647481>.
- Moll, P., Grossmann, L., Kutzli, I., Weiss, J., 2020. Influence of energy density and viscosity on foam stability—A study with pea protein (*Pisum Sativum* L.). *J. Dispers. Sci. Technol.* 41 (12), 1789–1796. <https://doi.org/10.1080/01932691.2019.1635028>.
- Mori, L., Mooney, M., Cha, M., 2018. Characterizing the influence of stress on foam conditioned sand for EPB tunneling. *Tunn. Undergr. Space Technol.* 71, 454–465. <https://doi.org/10.1016/j.tust.2017.09.018>.
- Peila, D., Oggeri, C., Borio, L., 2008. Influence of granulometry, time and temperature on soil conditioning for EPBS applications. *World Tunnel Congress 2008 - Underground Facilities for Better Environment and Safety* 3(1), 22–24.
- Peila, D., Martinelli, D., Todaro, C., Luciani, A., 2019. Soil conditioning in EPB shield tunnelling – An overview of laboratory tests. *Geomechanik Und Tunnelbau* 12 (5), 491–498. <https://doi.org/10.1002/GEOT.201900021>.
- Sebastiani, D., Vilardi, G., Bavasso, I., Di Palma, L., Miliziano, S., 2019. Classification of foam and foaming products for EPB mechanized tunnelling based on half-life time. *Tunn. Undergr. Space Technol.* 92 <https://doi.org/10.1016/J.TUST.2019.103044>.
- Thewes, M., Budach, C., 2010. Konditionierung von Lockergesteinen bei Erddruckschilden. *Geomechanik Und Tunnelbau (Transl.: Soil conditioning with foam during EPB tunnelling)* 3(3), 256–267. Doi: 10.1002/GEOT.201000023.
- Thewes, M., Budach, C., Bezuijen, A., 2012. Foam conditioning in EPB tunnelling. In: Viggiani, G. (Ed.), *Geotechnical Aspects of Underground Construction in Soft Ground* 1. CRC Press, pp. 127–135.
- Vinai, R., Peila, D., Oggeri, C., Pelizza, S., 2007. Laboratory tests for EPB tunnelling soil conditioning. In J. Barták, I. Hrdina, G. Romancov, & J. Zlámál (Eds.), *Underground Space—the 4th Dimension of Metropolises; Proceedings of the 33rd ITA-AITES World Tunnel Congress* 1(3), 273–278. Taylor & Francis Group.
- Wang, S., Ni, Z., Qu, T., Wang, H., Pan, Q., 2022. A novel index to evaluate the workability of conditioned coarse-grained soil for EPB shield tunnelling. *J. Constr. Eng. Manag.* 148 (6) [https://doi.org/10.1061/\(ASCE\)CO.1943-7862.0002287](https://doi.org/10.1061/(ASCE)CO.1943-7862.0002287).
- Wu, Y., Mooney, M.A., Cha, M., 2018. An experimental examination of foam stability under pressure for EPB TBM tunneling. *Tunn. Undergr. Space Technol.* 77, 80–93. <https://doi.org/10.1016/J.TUST.2018.02.011>.
- Yee, T. C., Marotta, M., Ow, C. N., 2018. Theory and Application of Excavation Management System for Slurry TBM in Singapore. *Underground Singapore*.
- Zhang, Y., Chang, Z., Luo, W., Gu, S., Li, W., An, J., 2015. Effect of starch particles on foam stability and dilational viscoelasticity of aqueous-foam. *Chin. J. Chem. Eng.* 23 (1), 276–280. <https://doi.org/10.1016/J.CJCHE.2014.10.015>.
- Zhao, S., Li, S., Wan, Z., Wang, X., Wang, M., Yuan, C., 2021. Effects of anti-clay agents on bubble size distribution and stability of aqueous foam under pressure for earth pressure balance shield tunneling. *Colloids Interface Sci. Commun.* 42 <https://doi.org/10.1016/J.COLCOM.2021.100424>.
- Zhou, X., Yang, Y., 2020. Effect of foam parameters on cohesionless soil permeability and its application to prevent the water spewing. *Appl. Sci. (Switzerland)* 10 (5). <https://doi.org/10.3390/APP10051787>.